Suppression of multiple ion bunches and generation of monoenergetic ion beams in laser foil-plasma*

Zhang Shan(张 闪)[a)b)], Xie Bai-Song(谢柏松)[a)†], Hong Xue-Ren(洪学仁)[a)c)], Wu Hai-Cheng(吴海城)[a)], Aimierding Aimidula(艾米尔丁·艾米都拉)[a)], Zhao Xue-Yan(赵学燕)[a)], and Liu Ming-Ping(刘明萍)[d)]

[a)] *College of Nuclear Science and Technology, Beijing Normal University, Beijing* 100875, *China*
[b)] *Department of Mathematics and Physics, Shijiazhuang Tiedao University, Shijiazhuang* 050043, *China*
[c)] *College of Physics and Electronic Engineering, Northwest Normal University, Lanzhou* 730070, *China*
[d)] *School of Information Engineering, Nanchang University, Nanchang* 330031, *China*

(Received 18 June 2010; revised manuscript received 12 July 2010)

In one-dimensional particle-in-cell simulations, this paper shows that the formation of multiple ion bunches is disadvantageous to the generation of monoenergetic ion beams and can be suppressed by choosing an optimum target thickness in the radiation pressure acceleration mechanism by a circularly polarised laser pulse. As the laser pulse becomes intense, the optimum target thickness obtained by a non-relativistic treatment is no longer adequate. Considering the relativistic Doppler-shifted pressure, it proposes a relativistic formulation to determine the optimum target thickness. The theoretical predictions agree with the simulation results well. The model is also valid for two-dimensional cases. The accelerated ion beams can be compelled to be more stable by choosing the optimum target thickness when they exhibit some unstable behaviours.

Keywords: interaction of ultrastrong laser pulse and plasma, radiation pressure acceleration, optimum target thickness

PACS: 52.38Kd, 52.65.Rr, 52.27.Ny **DOI:** 10.1088/1674-1056/20/1/015206

1. Introduction

Ion acceleration by ultrashort ultraintense laser pulse interacting with solid target has a great advance in the last decade. Some interesting experimental results were reported.[1−3] Several ion acceleration mechanisms of laser foil-plasma have been proposed.[4−8] Among them, the radiation pressure acceleration (RPA) has been highlighted as an efficient mechanism to accelerate large number of ions up to Giga-electron volts (GeV).[9] However, with a linearly polarised laser pulse, extremely high intensity at $I > 10^{23}$ W/cm^2 is required. With a circularly polarized (CP) laser pulse, the ponderomotive force has no oscillating component and the $\boldsymbol{J}\times\boldsymbol{B}$ heating is suppressed. The absence of hot electrons allows RPA to dominate at more moderate intensity. Therefore the RPA mechanism by a CP laser pulse is more promising for producing quasi-monoenergetic ion beams with not only high density but also high efficiency and low divergence.[9−23]

For RPA it has been shown that there are two distinct stages, i.e., hole-boring (HB) and light-sail (LS).[11,12,24] Recently, there are many works on the HB and the LS. For example, Macchi *et al.*[11] put forward a simple analytical model to account for the acceleration dynamics in the HB stage of RPA and provided scaling laws for the ion bunch energy and generation time as a function of laser intensity and plasma density. Also, the formation of multiple ion bunches in the HB stage was found.[13] By modifying the relativistic model, which was proposed by Zhang *et al.*,[17] Robinson *et al.*[24] derived a new set of fully relativistic formulae for the mean ion energy and HB velocity. More than one publication have shown that the LS stage can be well described by treating the plasma slab as a single object which perfectly reflects the incident light.[9,24] Qiao *et al.*[12] proposed a stable relativistic ion acceleration regime which depends critically on a smooth transition between the HB stage and the LS stage, and the high-density monoenergetic ion beams with energy above GeV and divergence

*Project supported by the National Natural Science Foundation of China (Grant Nos. 10875015, 10725521 and 10834008), and the National Basic Research Program of China (Grant No. 2006CB806004).
†Corresponding author. E-mail: bsxie@bnu.edu.cn
© 2011 Chinese Physical Society and IOP Publishing Ltd

of 10° are produced by two-dimensional (2D) simulations. In addition, the transverse instabilities in the LS stage of RPA and the effect of the laser spot profile on instabilities have been extensively studied.[23,25,26] Obviously, a thorough understanding of these issues is important for exploiting RPA mechanism.

The target thickness plays a crucial role in the RPA mechanism.[27,28] Yan *et al.*[18,29,31] have the opinion that if the laser field is larger than the maximum charge separation field, all electrons will be displaced, and the target is transparent to the laser pulse. Accordingly, they have given a criterion about the target thickness in order to make the overdense foil-plasma keep opaque to the laser pulse. Another target thickness is also obtained by the balance of the light pressure and electrostatic pressure acting on the compressed electron layer.[19,31] However, the relativistic effect is ignored. Just as the HB velocity is relativistically modified in Ref. [24], the target thickness should be modified similarly as the laser becomes intense.

In this paper, we use particle-in-cell (PIC) simulation to investigate the involving problems, especially the formation of multiple ion bunches in the HB stage and the effects on the quality of accelerated ion beams in the LS stage. It is found that the formation of the multiple ion bunches is disadvantageous to the generation of high quality ion beams in general conditions. The simulation results suggest that the generation of the multiple ion bunches can be suppressed by choosing the optimum target thickness which is strongly associated to the location of the wave breaking. As the laser pulse becomes intense, the optimum target thickness obtained by a non-relativistic treatment is no longer valid. A relativistic formula is proposed to determine the optimum target thickness by taking relativistic Doppler shift into account. Large number of one-dimensional (1D) PIC simulations have been performed in a wide range of foil density and laser intensity to verify the theoretical predictions and they are in excellent agreement with each other. This model is also valid for 2D cases. Especially we can compel the accelerated ion beams to be more stable by choosing the optimum target thickness when they exhibit some unstable behaviours.

2. Occurrence of wave breaking and influence of multiple ion bunches

The occurrence of wave breaking and the formation of multiple ion bunches can be seen in 1D PIC simulation. In our simulations, a CP laser pulse with $a_{\rm L} = 80$ along the x axis from left side is normally incident on a cold and pure hydrogen plasma slab with a step density $n_0 = 50n_{\rm c}$ and thickness $d = 2$ μm, where $a_{\rm L} = (eE_{\rm L}/m_{\rm e}\omega_{\rm L}c)$ is the normalized amplitude of a laser with electrical field $E_{\rm L}$ and carrier frequency $\omega_{\rm L}$, n_0 is the initial electron density, $n_{\rm c} = m_{\rm e}\omega_{\rm L}^2/4\pi e^2$ is the critical density, c is the speed of light in vacuum, $m_{\rm e}$ and e are the electron mass and elementary charge, respectively. The pulse profile of the laser field is given as $a_{\rm L}\exp[-(x-x_0)^{10}/2(c\tau_{\rm p})^{10}]$, where $x_0 = 10$ μm and $\tau_{\rm p} = 38$ fs. This pulse rises very rapidly to an intensity, $I_{\rm L}$, and stays approximately at the same intensity for 60 fs before falling. And in all simulations the laser impinges on the target at $t = 0$.

Figure 1 shows the snapshots of the electron and proton density profile, electrostatic field profile and proton phase space (x, $p_x/m_{\rm p}c$) projection at different moments. When the laser pulse impinges on the plasma, the electrons are quickly pushed inward by a large light pressure to pile up a compressed electron layer in front of the laser pulse and an electron depletion layer is left behind. In this process, it can be assumed that the ion-electron mass ratio M/m can be so large that the ions' inertia prevents the ions from moving significantly. From Fig. 1(a), we can clearly see the thin compressed electron layer and the almost motionless proton background. Additionally, the strong charge separation field E_x retains nearly linear profile in the electron depletion layer and the compressed electron layer (see Fig. 1(c)). A simple 1D model has been used to calculate electrostatic field profile.[11,18,31] Apart from the light pressure there is an electrostatic force, which is acting in the opposite direction on the compressed electron layer. At the initial stage of this process, the compressed electron layer is accelerated rapidly to a very large speed. And then, as the electrostatic force becomes strong, the compressed electron layer slows down. It is worthy of mentioning that the light pressure acting on the moving electron layer varies with the speed due to the Doppler-shift effect. Therefore, the light pressure increases as the speed of the compressed electron layer decreases. After a competitive process, a transient

equilibrium is reached.

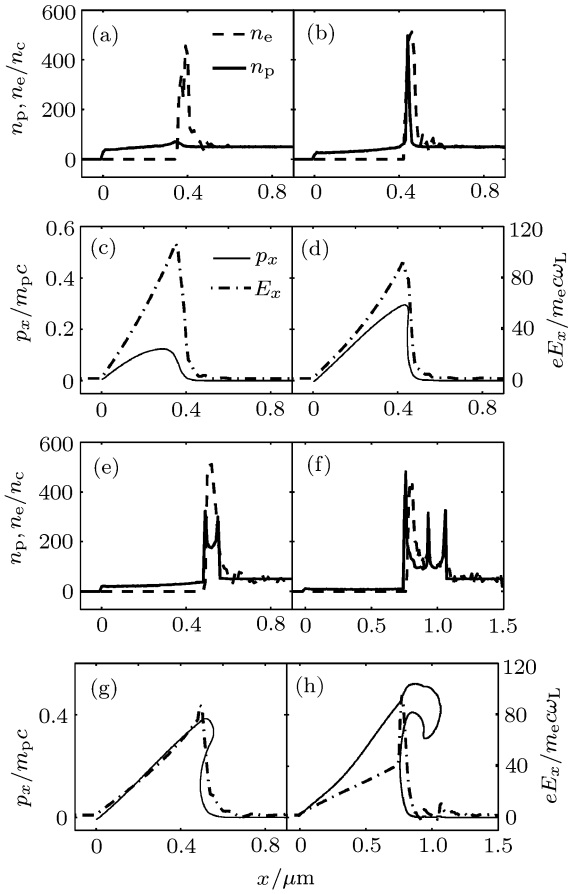


Fig. 1. Electron density profiles n_e/n_c (dashed lines), proton density profiles n_p/n_c (solid lines) at (a) $t = 3.2$ fs, (b) $t = 5.0$ fs, (e) $t = 6.2$ fs, and (f) $t = 11.0$ fs in the 1D PIC simulations. The (c), (d), (g) and (h) are the corresponding proton (x, p_x/m_pc) phase space projections (solid lines) and electrostatic field profiles $eE_x/m_ec\omega_L$ (dash-dot lines). Run parameters are $a_L = 80$, $n_0 = 50n_c$ and $d = 2$ μm.

Actually, as the transient equilibrium is reached, some ions have begun to move and their speed cannot be ignored any more. But the visible gathering has not taken place (see Fig. 1(a)). In view of the characteristics of the electrostatic field, more intense electric field should impart greater acceleration to the ions. So the ions near the field peak will catch up with those in the compressed electron layer. An ion density peak grows up as the ions gather constantly. We can see that the profile of velocity steepens in Fig. 1(d), and the first high-density ion spiking is formed in Fig. 1(b). On the next moment the wave breaking occurs. The location of wave breaking is near the rear surface of the electron layer in the state of transient equilibrium. The ions with greater speed will overtake the electron layer to form the second density ion spiking (see Fig. 1(e)). If the foil is not too thin and the pulse duration is not too short, the above-mentioned behaviours of ion gathering and wave breaking may occur several times in the whole laser–foil interaction processes. Finally the multiple ion bunches are formated. For example, three high-density ion bunches are formed in Fig. 1(f).

As the target becomes thicker, the faster ions overtake the compressed electron layer after the wave breaking happens. Because the big charge separation field exists only near the laser–foil interaction surface, once the accelerated ion bunches divorce from the compressed electron layer they will not be accelerated any more. If the profile of ion density is in the state of multiple ion bunches at the end of the HB stage, the ion beams will be accelerated in turn by the accelerating field in the LS stage. This will lead to low energy of the accelerated ion beams with wide energy spread and even multi ion energy peaks, in spite of large number of accelerated ions. In order that the ions have more chances to be accelerated by the accelerating field in the LS stage, the number of ion density spiking should be as less as possible. It is natural to think that the number of ion density spiking can be reduced by choosing thinner target. The effect of the target thickness on the quality of the accelerated ion beams can be seen in Fig. 2.

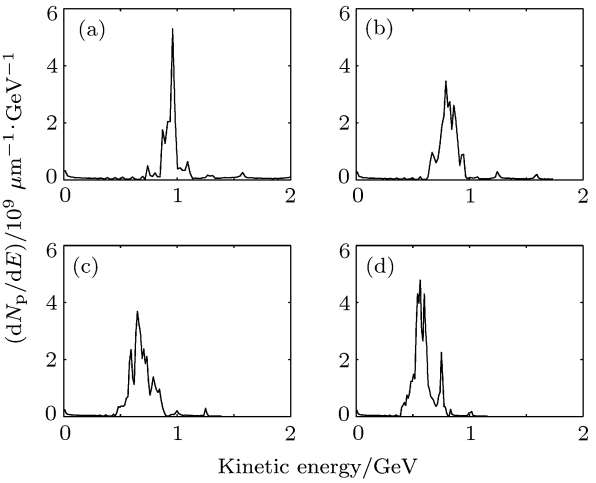


Fig. 2. The energy spectra of protons at $t = 117.2$ fs for the different target thickness: (a) $d = 0.44$ μm; (b) $d = 0.6$ μm; (c) $d = 0.8$ μm; (d) $d = 1.0$ μm. The other simulation parameters are the same as those in Fig. 1.

The energy spectra of accelerated proton beams are shown in Fig. 2 for different target thickness ($d = 0.44$, 0.6, 0.8 and 1.0 μm) at $t = 117.2$ fs, and the other simulation parameters are the same as those in Fig. 1. The target thickness $d = 0.44$ μm corresponds to the location of wave breaking in Fig. 1(b).

It can be found that the peak energy of accelerated proton beams decreases while the full-width-at-half-maximum (FWHM) increases as the target becomes thicker. Furthermore, the multi energy peaks can be seen in Fig. 2(d). Accordingly, the optimum target thickness should coincide with the location of wave breaking in order to attain higher energetic ion beams with lower energy spread.

3. Relativistically modified target thickness

The present simulation results show that the target thickness plays a crucial role in the formation of multiple ion bunches. The multiple ion bunches can be suppressed if we properly choose the optimum target thickness, which coincides with the location of the wave breaking. By aforementioned considerations of the dynamics of laser–foil interaction and large number of simulations, we can obtain that the location of wave breaking is near the back surface of the compressed electron layer which is at the transient equilibrium. Thus the optimum target thickness, d, can be calculated as $d = d_{\rm i} + l_{\rm s}$, where $d_{\rm i}$ is the thickness of the electron depletion layer and $l_{\rm s}$ is the compressed electron layer. By large number of simulations, we find that the thickness of the compressed electron layer remains approximately equal to the skin depth or the relativistic skin depth i.e., $l_{\rm s} \sim c/\omega_{\rm p} \sim \sqrt{\gamma}c/\omega_{\rm p}$. Usually the thickness of the compressed electron layer is much less than that of the electron depletion layer, the thickness of the compressed electron layer can be neglected. Thus the optimum target thickness can be calculated approximately as $d \simeq d_{\rm i}$.

On the basis of the balance between the light pressure, $2I_{\rm L}/c$, and electrostatic pressure, $E_0^2/8\pi$, acting on the compressed electrons layer, the thickness of the electron depletion layer, $d_{\rm i}$, is usually calculated as[11,18,23,31]

$$E_0^2/8\pi = 2I_{\rm L}/c, \tag{1}$$

where $E_0 = 4\pi e n_0 d_{\rm i}$ is the peak value of the space charge field E_x in the transient equilibrium. Here, it is assumed that the laser pulse is completely reflected. A series of PIC simulations were carried out for different laser intensity and plasma density. A series of maximum electrostatic fields obtained in PIC simulations and Eq. (1) are plotted respectively in Figs. 3(a), 3(b) and 3(c), where E_0 is normalized by $e/m_{\rm e}c\omega_{\rm L}$. It is clear that the results of simulations agree poorly with those of Eq. (1) as the laser becomes intense. Furthermore, the thickness of electron depletion layer in Eq. (1) and PIC simulation are also plotted respectively in Figs. 3(d), 3(e) and 3(f). As can be seen, the results of simulations agree poorly with those of Eq. (1) as the laser becomes intense. Therefore, as the laser becomes intense, Eq. (1) is not valid.

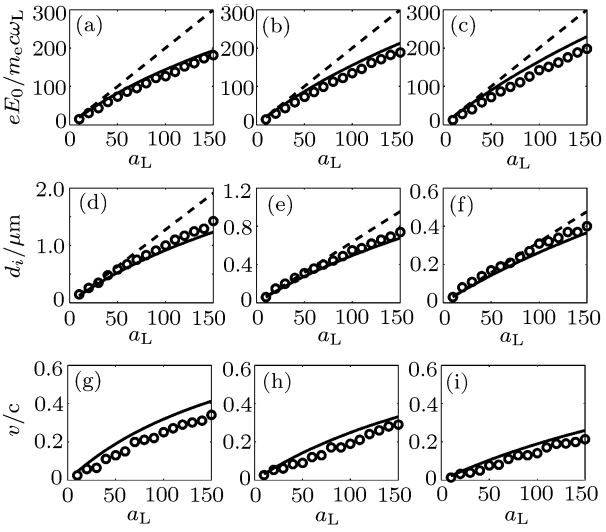


Fig. 3. Plots (circles) of the maximum electrostatic fields, the thickness of the electron depletion layer and the average velocity of the electron layer at the transient equilibrium in the PIC simulations for (a), (d) and (g) $n_0 = 25n_{\rm c}$, (b), (e) and (h) $n_0 = 50n_c$, (c), (f) and (i) $n_0 = 100n_c$. The values of $a_{\rm L}$ are selected at intervals, 10, between 10 and 150. Predictions of Eq. (1) (dashed lines) and Eq. (2) (solid lines) in (a)–(f). And predictions of the relativistic HB velocity in Ref. [19] (solid lines) in (g), (h) and (i).

Considering that the compressed electron layer is moving forward and the relativistic Doppler shift happens, the light pressure acting on the compressed electron layer will become smaller. Assuming that the laser pulse is completely reflected, we can modify the light pressure as $(2I_{\rm L}/c)(c - v_{\rm f})/(c + v_{\rm f})$, where $v_{\rm f}$ is the velocity of the compressed electron layer. This result follows from the relativistic Doppler shift and the conservation of photon number.[19,24] Thus one can proceed to write down the modified expression of the pressure balance equation as

$$E_0^2/8\pi = \frac{2I_{\rm L}}{c}\left(\frac{c - v_{\rm f}}{c + v_{\rm f}}\right). \tag{2}$$

In the preceding discussion it is known that some ions have begun to move. In other words, the large electrostatic shock has been formed and the balance between the light pressure and the momentum flux of the ions in Refs. [17] and [24] is suitable. So the velocity of

the compressed electron layer, $v_{\rm f}$, should be approximately equal to the relativistic HB velocity $v_{\rm b}$,[24] i.e., $v_{\rm f} \approx v_{\rm b} = \sqrt{I_{\rm L}/m_{\rm i}n_{\rm i}c^3}/(1+\sqrt{I_{\rm L}/m_{\rm i}n_{\rm i}c^3})$, $m_{\rm i}$ and $n_{\rm i}$ are the ion mass and density respectively. In order to verify this prediction, the average speed $v_{\rm f}$ of the compressed electron layer in the transient equilibrium is plotted against the relativistic HB velocity $v_{\rm b}$ in Figs. 3(g), 3(h) and 3(i). As can be seen, there is a good agreement between $v_{\rm f}$ and $v_{\rm b}$. For the maximum electrostatic field and the thickness of electron depletion layer, the results of Eq. (2) are also compared with those of Eq. (1) and PIC simulation in Fig. 3. It can be seen that the results of Eq. (2) agree better with those of PIC simulation than those of Eq. (1), especially as the laser becomes intense.

A series of PIC simulations are also carried out by using the different target thickness in Eqs. (1) and (2) respectively. The peak energy and the energy spread of accelerated proton beams are calculated at 117.2 fs for all simulations. And they are plotted in Fig. 4. Using the target thickness in Eq. (2), we find that the peak energy is even higher and the energy spread is even lower than the results of the unmodified theory, especially as the laser becomes intense.

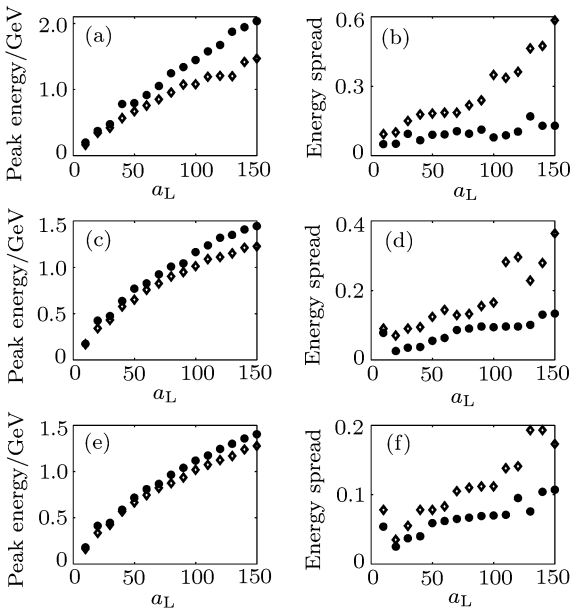


Fig. 4. Plots of the peak energy and the energy spread of the accelerated proton beams at $t = 117.2$ fs in the PIC simulations for (a) and (b) $n_0 = 25n_c$, (c) and (d) $n_0 = 50n_c$, (e) and (f) $n_0 = 100n_c$. The values of $a_{\rm L}$ are selected at intervals, 10, between 10 and 150. The filled circle and the square are the results in simulations for the target thickness given by the modified theory and the unmodified theory respectively.

4. Two-dimensional simulations

The results obtained so far are based on 1D PIC simulation. However, real experiments are always multidimensional. Our model is also valid for 2D cases. In our 2D simulations, a grid of 5100 cells along the laser axis and 4000 cells transversely (51 μm×40 μm) is used. The spatial profile of the laser field is given as $a_{\rm L}\exp(-r^4/2r_0^4)\exp[-(x-x_0)^{10}/2(c\tau_{\rm p})^{10}]$, where $r_0 = 10$ μm, $x_0 = 10$ μm and $\tau_{\rm p} = 38$ fs. For $a_{\rm L} = 80$ and $n_0 = 50n_{\rm c}$, we choose $d \approx 0.44$ μm according to our model. The simulation results at $t = 117.2$ fs are shown in Fig. 5. The proton density $n_{\rm p}/n_{\rm c}$ and phase space distribution $(x, p_x/m_{\rm p}c)$ in Figs. 5(a) and 3(c) show that the high-density ($40n_{\rm c}$), high-quality relativistic proton beams ($2m_{\rm i}c$ momentum) have been generated. The energy spectra of GeV proton beams by stable acceleration are shown in Fig. 5(b). The proton beams have a peak energy of about 1.1 GeV with the energy spread $\sim 13\%$. Figure 5(d) shows the proton energy distribution as a function of the divergent angle. The high quality proton beams with opening angle $\sim 5^\circ$ corresponding to the proton 'head' in Fig. 5(c) are obtained.

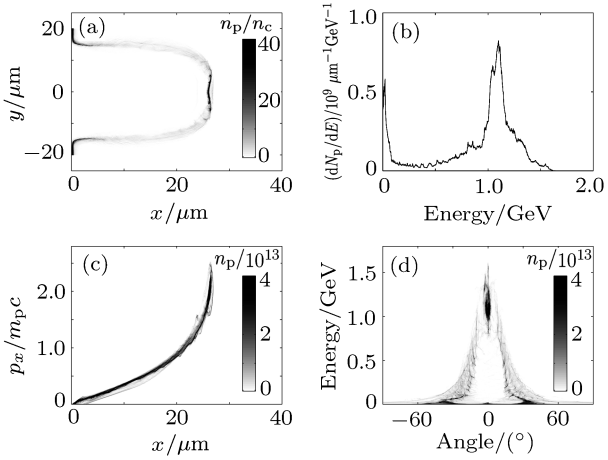


Fig. 5. Results in the 2D PIC simulations. The parameters are $a_{\rm L} = 80$, $n_0 = 50n_{\rm c}$, $d = 0.44\mu$m and $t = 117.2$ fs. (a) Proton density $n_{\rm p}/n_{\rm c}$ in the (x, y) plane. (b)Proton energy spectra in the region of $|y| < 10$ μm. The (c) and (d) show the proton phase space distribution (x, p_x) and the proton energy distribution as a function of the divergent angle respectively.

Especially we can compel the accelerated ion beams to be more stable by choosing the modified target thickness when the accelerated ions exhibit some unstable behaviours. We choose two examples of the unstable acceleration in Ref. [12]. For $a_{\rm L} = 82.9$, $n_0 = 100n_{\rm c}$ and $a_{\rm L} = 26.2$, $n_0 = 30n_{\rm c}$, we obtain

$d = 0.25$ μm and $d = 0.29\mu$m respectively according to the modified theory. The stable acceleration cases can be obtained (see Figs. 6(a) and 6(c)). Corresponding to the two cases, it can be seen from Figs. 6(b) and 6(d) that the energetic proton beams have the peak energy of about 1.0 GeV with the energy spread $\sim 20\%$ and 0.6 GeV with the energy spread $\sim 24\%$ respectively, and the opening angle $\sim 5^\circ$. Additionally, we also find that the transverse super Gaussian pulse profile and larger laser spot seem more advantageous to achieve more narrowly peaked spectra.

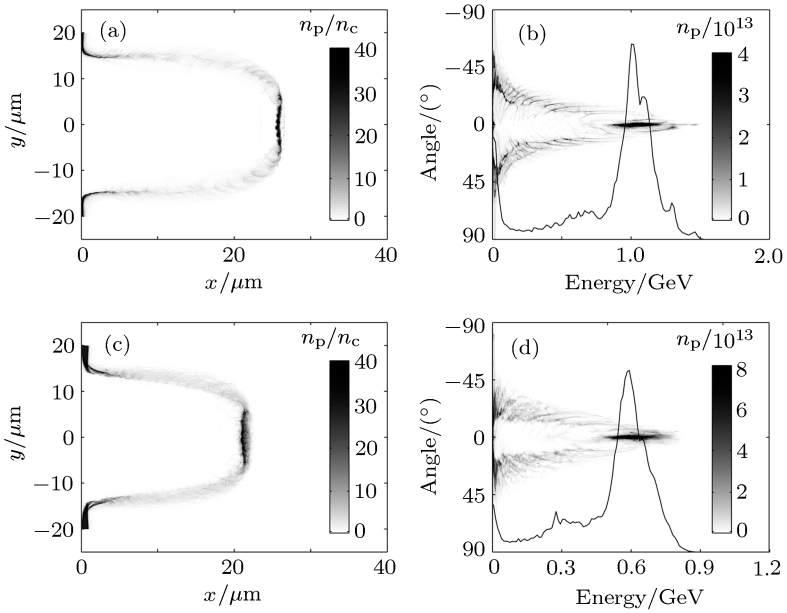


Fig. 6. Results in 2D PIC simulations. Proton density n_p/n_c in (a), energy distribution in (b) at $t = 117.2$ fs for the foil of $n_0 = 100n_c$, $d = 0.25$ μm at $a_L = 82.9$. The (c) and (d) show another case with $a_L = 26.2$, $n_0 = 30n_c$ and $d = 0.29$ μm.

5. Summary and discussions

In summary, we investigate the effect of multiple ion bunches by PIC simulation. It is disadvantageous to the formation of the high quality ion beams. Our study shows that the generation of the multiple ion bunches can be suppressed by choosing the optimum target thickness, which is strongly associated to the location of the wave breaking. As the laser becomes intense the optimum target thickness obtained from a non-relativistic treatment is no longer valid. Then, we propose a relativistically formula to calculate the optimum target thickness by considering the relativistic Doppler shift. The results of PIC simulation have confirmed the theoretical prediction. Additionally, we can compel the accelerated ion beams to be more stable by choosing the optimum target thickness when they exhibit some unstable behaviours.

Our simulation results have also shown that the quality of the accelerated ion beams becomes poorer as the target becomes thicker. However, one can obtain narrower energy spread and higher maximum energy if only the laser pulse duration is long enough. On the other hand, in order to obtain the same quality of the accelerated ion beams, thicker the target is, lower the proportion of accelerated ions is, which means that the efficiency of energy transfer from the laser pulse to plasma becomes lower as the target becomes thicker. Therefore the competition and optimum conditions among them need to be researched furthermore in generation of monoenergetic ion beams with low spatial divergence by ultraintense laser pulse interacting with foil-plasma.

References

[1] Maksimchuk A, Gu S, Flippo K and Umstadter D 2000 *Phys. Rev. Lett.* **84** 4108

[2] Clark E L, Krushelnick K, Zepf M, Beg F N, Tatarakis M, Machacek A, Santala M I K, Watts I, Norreys P A and Dangor A E 2000 *Phys. Rev. Lett.* **85** 1654

[3] Snavely R A, Key M H, Hatchett S P, Cowan T E, Roth M, Phillips T W, Stoyer M A, Henry E A, Sangster T C, Singh M S, Wilks S C, MacKinnon A, Offenberger A, Pennington D M, Yasuike K, Langdon A B, Lasinski B F, Johnson J, Perry M D and Campbell E M 2000 *Phys. Rev. Lett.* **85** 2945
[4] Wilks S C, Langdon A B, Cowan T E, Roth M, Singh M, Hatchett S, Key M H, Pennington D, MacKinnon A and Snavely R A 2001 *Phys. Plasmas* **8** 542
[5] Silva L O, Marti M, Davies J R, Fonseca R A, Ren C, Tsung F S and Mori W B 2004 *Phys. Rev. Lett.* **92** 015002
[6] Shen B F and Xu Z Z 2001 *Phys. Rev.* E **64** 056406
[7] Liu M P, Wu H C, Xie B S, Hong X R, Zhang S and Yu M Y 2009 *Phys. Plasmas* **16** 083104
[8] He M Q, Dong Q L, Sheng Z M, Weng S M, Chen M, Wu H C and Zhang J 2009 *Acta Phys. Sin.* **58** 363 (in Chinese)
[9] Esirkepov T, Borghesi M, Bulanov S V, Mourou G and Tajima T 2004 *Phys. Rev. Lett.* **92** 175003
[10] Geng S F, Tang D L, Zhao J and Qiu X M 2009 *Acta Phys. Sin.* **58** 5520 (in Chinese)
[11] Macchi A, Cattani F, Liseykina T V and Cornolti F 2005 *Phys. Rev. Lett.* **94** 165003
[12] Qiao B, Zepf M, Borghesi M and Geissler M 2009 *Phys. Rev. Lett.* **102** 145002
[13] Macchi A, Veghini S and Pegoraro F 2009 *Phys. Rev. Lett.* **103** 085003
[14] Jin Z Y, Shen B F, Zhang X M, Wang F C and Ji L L 2009 *Chin. Phys.* B **18** 5395
[15] Chen M, Sheng Z M, Zheng J and Zhang J 2006 *Acta Phys. Sin.* **55** 2381 (in Chinese)
[16] Chen M, Sheng Z M and Zhang J 2006 *Chin. Phys.* **15** 568
[17] Zhang X M, Shen B F, Li X M, Jin Z Y and Wang F C 2007 *Phys. Plasmas* **14** 073101
[18] Yan X Q, Lin C, Sheng Z M, Guo Z Y, Liu B C, Lu Y R, Fang J X and Chen J E 2008 *Phys. Rev. Lett.* **100** 135003
[19] Tripathi V K, Liu C S, Shao X, Eliasson B and Sagdeev R Z 2009 *Plasma Phys. Control. Fusion* **51** 024014
[20] Liseikina T V and Macchi A 2007 *Appl. Phys. Lett.* **91** 171502
[21] Robinson A P L, Zepf M, Kar S, Evans R G and Bellei C 2008 *New J. Phys.* **10** 013021
[22] Macchi A, Liseikina T V, Tuveri S and Veghini S 2009 *C. R. Physique* **10** 207
[23] Klimo O, Psikal J, Limpouch J and Tikhonchuk V T 2008 *Phys. Rev. ST Accel Beams* **11** 031301
[24] Robinson A P L, Gibbon P, Zepf M, Kar S, Evans R G and Bellei C 2009 *Plasma Phys. Control. Fusion* **51** 024004
[25] Pegoraro F and Bulanov S V 2007 *Phys. Rev. Lett.* **99** 065002
[26] Chen M, Pukhov A, Sheng Z M and Yan X Q 2008 *Phys. Plasmas* **15** 113103
[27] Henig A, Steinke S, Schnürer M, Sokollik T, Hörlein R, Kiefer D, Jung D, Schreiber J, Hegelich B M, Yan X Q, Meyer-ter-Vehn J, Tajima T, Nickles P V, Sandner W and Habs D 2009 *Phys. Rev. Lett.* **103** 245003
[28] Eliasson B, Liu C S, Shao X, Sagdeev R Z and Shukla P K 2009 *New J. Phys.* **10** 073006
[29] Yan X Q, Lin C, Sheng Z M, Guo Z Y, Liu B C, Lu Y R, Fang J X and Chen J E 2009 *Phys. Rev. Lett.* **102** 239502
[30] Ji L L, Shen B F, Zhang X M, Wang F C, Jin Z Y, Wen M, Wang W P and Xu J C 2009 *Phys. Rev. Lett.* **102** 239501
[31] Yin Y, Yu W, Yu M Y, Lei A, Yang X Q, Xu H and Senecha V K 2008 *Phys. Plasmas* **15** 093106